

# Tailoring spin-orbit torque in diluted magnetic semiconductors

Hang Li, Xuhui Wang, Fatih Doğan, and Aurelien Manchon\*  
 King Abdullah University of Science and Technology (KAUST),  
 Physical Science and Engineering Division, Thuwal 23955-6900, Saudi Arabia  
 (Dated: July 20, 2018)

We study the spin orbit torque arising from an intrinsic *linear* Dresselhaus spin-orbit coupling in a single layer III-V diluted magnetic semiconductor. We investigate the transport properties and spin torque using the linear response theory and we report here : (1) a strong correlation exists between the angular dependence of the torque and the anisotropy of the Fermi surface; (2) the spin orbit torque depends nonlinearly on the exchange coupling. Our findings suggest the possibility to tailor the spin orbit torque magnitude and angular dependence by structural design.

PACS numbers: 72.25.Dc, 72.20.My, 75.50.Pp

The electrical manipulation of magnetization is central to spintronic devices such as high density magnetic random access memory,<sup>1</sup> for which the spin transfer torque provides an efficient magnetization switching mechanism.<sup>2,3</sup> Beside the conventional spin-transfer torque, the concept of spin-orbit torque in both metallic systems and diluted magnetic semiconductors (DMS) has been studied theoretically and experimentally.<sup>4-9</sup> In the presence of a charge current, the spin-orbit coupling produces an effective magnetic field which generates a non-equilibrium spin density that in turn exerts a torque on the magnetization.<sup>4-6</sup> Several experiments on magnetization switching in strained (Ga,Mn)As have provided strong indications that such a torque can be induced by a Dresselhaus-type spin-orbit coupling, achieving critical switching currents as low as  $10^6$  A/cm<sup>2</sup>.<sup>7-9</sup> However, up to date very few efforts are devoted to the nature of the spin-orbit torque in such a complex system and its magnitude and angular dependence remain unaddressed.

In this Letter, we study the spin-orbit torque in a diluted magnetic semiconductor submitted to a linear Dresselhaus spin-orbit coupling. We highlight two effects that have not been discussed before. First, a strong correlation exists between the angular dependence of the torque and the anisotropy of the Fermi surface. Second, the spin torque depends *nonlinearly* on the exchange coupling. To illustrate the flexibility offered by DMS in tailoring the spin-orbit torque, we compare the torques obtained in two stereotypical materials, (Ga,Mn)As and (In,Mn)As.

The system under investigation is a uniformly magnetized single domain DMS film made of, for example, (Ga,Mn)As or (In,Mn)As. We assume the system is well below its critical temperature. An electric field is applied along the  $\hat{x}$  direction. It is worth pointing out that we consider here a large-enough system to allow us disregard any effects arising due to boundaries and confinement.

We use the *six-band* Kohn-Luttinger Hamiltonian to

describe the band structure of the DMS,<sup>9</sup>

$$H_{\text{KL}} = \frac{\hbar^2}{2m} \left[ (\gamma_1 + \frac{5}{2}\gamma_2)k^2 - 2\gamma_3(\mathbf{k} \cdot \hat{\mathbf{J}})^2 + 2(\gamma_3 - \gamma_2) \sum_i k_i^2 \hat{J}_i^2 \right]. \quad (1)$$

where the phenomenological Luttinger parameters  $\gamma_{1,2,3}$  determine the band structure and the effective mass of valence-band holes.  $\gamma_3$  is the anisotropy parameter,  $\hat{\mathbf{J}}$  is the total angular momentum and  $k$  is the wave vector. The bulk inversion asymmetry allows us to augment the Kohn-Luttinger Hamiltonian by a strain-induced spin-orbit coupling of the Dresselhaus type.<sup>5,7</sup> We assume the growth direction of (Ga,Mn)As is directed along the  $z$ -axis, two easy axes are pointed at  $x$  and  $y$ , respectively.<sup>10</sup> In this case, the components of the strain tensor  $\epsilon_{xx}$  and  $\epsilon_{yy}$  are identical. Consequently, we may have a linear Dresselhaus spin-orbit coupling<sup>7</sup>

$$H_{\text{DSOC}} = \beta(\hat{\sigma}_x k_x - \hat{\sigma}_y k_y), \quad (2)$$

given  $\beta$  the coupling constant that is a function of the axial strain.<sup>7,11</sup>  $\hat{\sigma}_{x(y)}$  is the  $6 \times 6$  spin matrix of holes and  $k_{x(y)}$  is the wave vector.

In the DMS systems discussed here, we incorporate a mean-field like exchange coupling to enable the spin angular momentum transfer between the hole spin ( $\hat{\mathbf{s}} = \hbar\hat{\boldsymbol{\sigma}}/2$ ) and the localized ( $d$ -electron) magnetic moment  $\hat{\boldsymbol{\Omega}}$  of ionized Mn<sup>2+</sup> acceptors,<sup>12,13</sup>

$$H_{\text{ex}} = 2J_{\text{pd}} N_{\text{Mn}} S_a \hat{\boldsymbol{\Omega}} \cdot \hat{\mathbf{s}} / \hbar \quad (3)$$

where  $J_{\text{pd}}$  is the antiferromagnetic coupling constant.<sup>13,14</sup> Here  $S_a = 5/2$  is the spin of the acceptors. The hole spin operator, in the present six-band model, is a  $6 \times 6$  matrix.<sup>13</sup> The concentration of the ordered local Mn<sup>2+</sup> moments  $N_{\text{Mn}} = 4x/a^3$  is given as a function of  $x$  that defines the doping concentration of Mn ion.  $a$  is the lattice constant. Therefore, the entire system is described by the total Hamiltonian

$$H_{\text{sys}} = H_{\text{KL}} + H_{\text{ex}} + H_{\text{DSOC}}. \quad (4)$$

In order to calculate the spin torque, we determine the nonequilibrium spin densities  $\mathbf{S}$  (of holes) as a *linear* response to an external electric field,<sup>5</sup>

$$\mathbf{S} = eE_x \frac{1}{V} \sum_{n,\mathbf{k}} \frac{1}{\hbar\Gamma_{n,\mathbf{k}}} \langle \hat{\mathbf{v}} \rangle \langle \hat{\mathbf{s}} \rangle \delta(E_{n,\mathbf{k}} - E_F). \quad (5)$$

where  $\hat{\mathbf{v}}$  is the velocity operator. In Eq.(5), the scattering rate of hole carriers by Mn ions is obtained by Fermi's golden rule,<sup>12</sup>

$$\Gamma_{n,\mathbf{k}}^{\text{Mn}^{2+}} = \frac{2\pi}{\hbar} N_{\text{Mn}} \sum_{n'} \int \frac{d\mathbf{k}'}{(2\pi)^3} |M_{n,n'}^{\mathbf{k},\mathbf{k}'}|^2 \times \delta(E_{n,\mathbf{k}} - E_{n',\mathbf{k}'})(1 - \cos\phi_{\mathbf{k},\mathbf{k}'}), \quad (6)$$

where  $\phi_{\mathbf{k},\mathbf{k}'}$  is the angle between two wave vectors  $\mathbf{k}$  and  $\mathbf{k}'$ . The matrix element  $M_{n,n'}^{\mathbf{k},\mathbf{k}'}$  between two eigenstates  $(\mathbf{k}, n)$  and  $(\mathbf{k}', n')$  is

$$M_{n,n'}^{\mathbf{k},\mathbf{k}'} = J_{\text{pd}} S_a \langle \psi_{n\mathbf{k}} | \hat{\mathbf{\Omega}} \cdot \hat{\mathbf{s}} | \psi_{n'\mathbf{k}'} \rangle - \frac{e^2}{\epsilon(|\mathbf{k} - \mathbf{k}'|^2 + p^2)} \langle \psi_{n\mathbf{k}} | \psi_{n'\mathbf{k}'} \rangle. \quad (7)$$

Here  $\epsilon$  is the dielectric constant of the host semiconductors and  $p = \sqrt{e^2 g / \epsilon}$  is the Thomas-Fermi screening wave vector, where  $g$  is the density of states at Fermi level. Finally, we calculate the field like spin-orbit torque using<sup>4</sup>

$$\mathbf{T} = J_{\text{ex}} \mathbf{S} \times \hat{\mathbf{\Omega}}, \quad (8)$$

where  $J_{\text{ex}} \equiv J_{\text{pd}} N_{\text{Mn}} S_a$ . Throughout this Letter, the results are given in terms of the torque efficiency  $\mathbf{T}/eE$ . The interband transitions, arising from distortions in the distribution function induced by the applied electric field, are neglected in our calculation. This implies that the torque extracted from the present model is expected to accommodate only a field-like component. The above protocols based on linear response formalism allow us to investigate the spin-orbit torque for a wide range of DMS material parameters.

We plot in Fig.1(a) the spin torque as a function of the magnetization angle for different values of the band structure anisotropy parameter  $\gamma_3$ . The topology of the Fermi surface can be modified by a linear combination of  $\gamma_2$  and  $\gamma_3$ : if  $\gamma_2 = \gamma_3 \neq 0$ , the Fermi surface around the  $\Gamma$  point is spherical, as shown in Fig.1(c). In this special case, the angular dependence of the torque is simply proportional to  $\cos\theta$  [red curve in Fig.1(a)], as expected from the symmetry of the  $k$ -linear Dresselhaus Hamiltonian, Eq. (2)<sup>4</sup>. When  $\gamma_3 \neq \gamma_2$ , the Fermi surface deviates from a sphere [Fig.1(b) and (d)] and, correspondingly, the angular dependence of the torque deviates from a simple  $\cos\theta$  function [i.e., curves corresponding to  $\gamma_3 = 1.0$  and  $\gamma_3 = 2.93$  in Fig.1(a)]. In a comparison to the spherical case, the maximal value of the torque at  $\theta = 0$  is lower for  $\gamma_3 \neq \gamma_2$ . As Eq.(5) indicates, in the linear response treatment formulated here, the magnitude of the spin torque is determined by the transport scattering time

and the expectation values of spin and velocity operators of holes. Qualitatively, as the Fermi surface deviates from a sphere, the expectation value  $\langle \hat{s}_x \rangle$  of the heavy hole band, contributing the most to the spin torque, is lowered at  $\theta = 0$ .

More specifically, as the Fermi surface warps, the angular dependence of the spin torque develops, in addition to the  $\cos\theta$  envelop function, an oscillation with a period that is shorter than  $\pi$ . The period of these additional oscillations increases as the Fermi surface becomes more anisotropic in  $k$ -space, see Fig. 1(b) and (d). To further reveal the effect of band warping on spin torque, we plot  $T_y / \cos\theta$  as a function of the magnetization angle in inset of Fig.1(a). When  $\gamma_3 = 2.0$  (spherical Fermi sphere),  $T_y / \cos\theta$  is a constant, for  $T \propto \cos\theta$ . When  $\gamma_3 = 2.93$  or 1.0, the transport scattering time of the hole carriers starts to develop an oscillating behavior in  $\theta$ ,<sup>15</sup> which eventually contributes to additional angular dependencies in the spin torque. The angular dependencies in spin-orbit torque shall be detectable by techniques such as spin-FMR<sup>9</sup>.

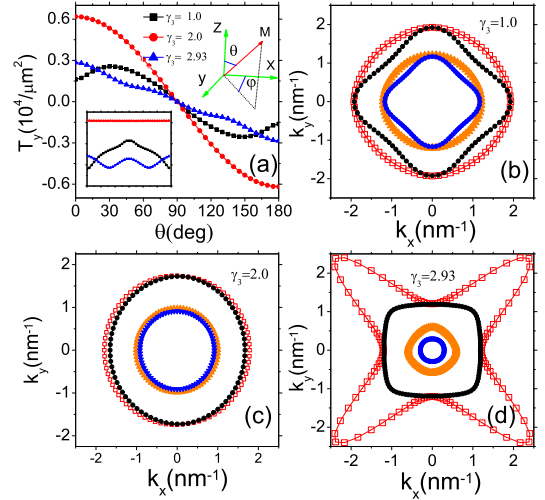


FIG. 1. (Color online) (a) The  $y$ -component of the spin torque as a function of magnetization direction. Fermi surface intersection in the  $k_z = 0$  plane for (b)  $\gamma_3 = 1.0$ , (c)  $\gamma_3 = 2.0$  and (d)  $\gamma_3 = 2.93$ . The red, black, orange and blue contours stands for majority heavy hole, minority heavy hole, majority light hole and minority light hole band, respectively. Inset (a) depicts  $T_y / \cos\theta$  as a function of magnetization direction. The others parameters are  $(\gamma_1, \gamma_2) = (6.98, 2.0)$ ,  $J_{\text{pd}} = 55 \text{ meV nm}^3$  and  $p = 0.2 \text{ nm}^{-3}$ .

In Fig.2, we compare the angular dependence of spin torque ( $T_y$ ) for both (Ga,Mn)As and (In,Mn)As which are popular materials in experiments and device fabrication.<sup>16-18</sup> Although (In,Mn)As is, in terms of exchange coupling and general magnetic properties, rather similar to (Ga,Mn)As, the difference in band structures, lattice constants, and Fermi energies between these two materials gives rise to different density of states, strains, and transport scattering rates. For both materials, the

spin torque decrease monotonically as the angle  $\theta$  increases from 0 to  $\pi/2$ . Throughout the entire angle range  $[0, \pi]$ , the amplitude of the torque in (In,Mn)As is twice larger than that in (Ga,Mn)As. We mainly attribute this to two effects. First of all, the spin-orbit coupling constant  $\beta$  in (In,Mn)As is about twice as larger than that in (Ga,Mn)As. Second, for the same hole concentration, the Fermi energy of (In,Mn)As is higher than that of (Ga,Mn)As.

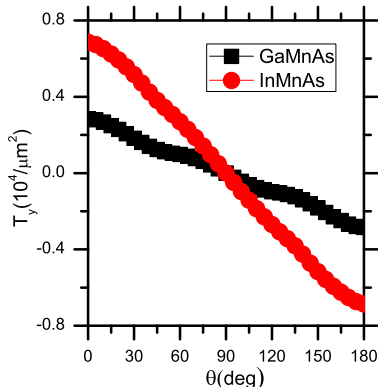


FIG. 2. (Color online) Torque  $T_y$  as a function of the magnetization direction for (Ga,Mn)As (black square) and (In,Mn)As (red dots). For (Ga,Mn)As,  $(\gamma_1, \gamma_2, \gamma_3) = (6.98, 2.0, 2.93)$ ; for (In,Mn)As,  $(\gamma_1, \gamma_2, \gamma_3) = (20.0, 8.5, 9.2)$ . The strength of the spin-orbit coupling constant is: for (Ga,Mn)As,  $\beta = 1.6$  meV nm; for (In,Mn)As,  $\beta = 3.3$  meV nm.<sup>19</sup> The exchange coupling constant  $J_{\text{pd}} = 55$  meV nm<sup>3</sup> for (Ga,Mn)As<sup>20</sup> and 39 meV nm<sup>3</sup> for (In,Mn)As.<sup>21</sup>

In the following, we further demonstrate a counter-intuitive feature that, in the DMS system considered in this Letter, the spin orbit torque depends nonlinearly on the exchange splitting. In Fig. 3(a),  $T_y$  component of the spin torque is plotted as a function of the exchange coupling  $J_{\text{pd}}$ , for different values of  $\beta$ . In the weak exchange coupling regime, the electric generation of non equilibrium spin density dominates, then the leading role of exchange coupling is defined by its contribution to the transport scattering rate. We provide a simple qualitative explanation on such a peculiar  $J_{\text{pd}}$  dependence. Using a Born approximation, the scattering rate due to the  $p-d$  interaction is proportional to  $1/\tau_J = bJ_{\text{pd}}^2$ , where parameter  $b$  is  $J_{\text{pd}}$ -independent. When the nonmagnetic scattering rate  $1/\tau_0$  is taken into account, i.e., the Coulomb interaction part in Eq.(7), the total scattering time in Eq.(5) can be estimated as

$$\frac{1}{\hbar\Gamma} \propto \frac{1}{bJ_{\text{pd}}^2 + \frac{1}{\tau_0}}, \quad (9)$$

which contributes to the torque by  $T \propto J_{\text{pd}}/(\hbar\Gamma)$ . This explains the transition behavior, i.e., increases linearly then decreases, in the moderate  $J_{\text{pd}}$  regime in Fig.3. As the exchange coupling further increases, Eq.(9) is dominated by the spin-dependent scattering, therefore the

scattering time  $1/\hbar\Gamma \propto 1/J_{\text{pd}}^2$ . Meanwhile, the energy splitting due to the exchange coupling becomes significant, thus  $\langle \hat{s} \rangle \propto J_{\text{pd}}$ . In total, the spin torque is insensitive to  $J_{\text{pd}}$ , explaining the flat curve in the large exchange coupling regime. In Fig. 3(b), we plot the influence of the exchange coupling on the spin torque for two materials. In (In,Mn)As, mainly due to a larger Fermi energy in a comparison to (Ga,Mn)As, the peak of the spin torque shifts towards a larger  $J_{\text{pd}}$ . The dependence of the torque as a function of the exchange in (In,Mn)As is more pronounced than in (Ga,Mn)As, due to a stronger spin-orbit coupling.

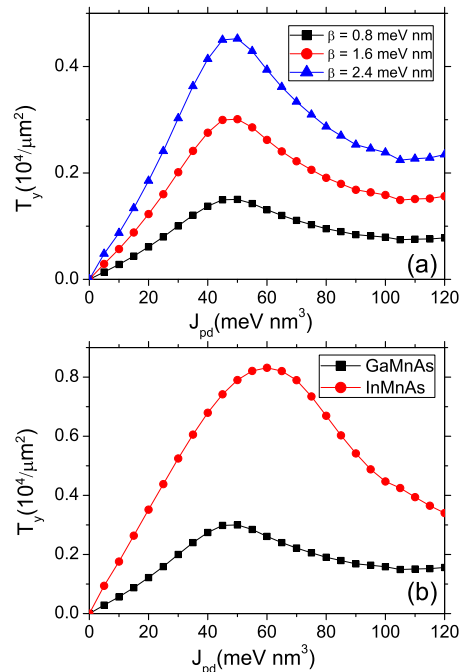


FIG. 3. (Color online) The  $T_y$  component of the spin torque as a function of exchange coupling  $J_{\text{pd}}$ . (a)  $T_y$  versus  $J_{\text{pd}}$  at various values of  $\beta$ , for (Ga,Mn)As. (b)  $T_y$  versus  $J_{\text{pd}}$ , for both (Ga,Mn)As and (In,Mn)As. The magnetization is directed along the  $z$ -axis ( $\theta = 0$ ). The other parameters are the same as those in Fig.2.

The possibility to engineer electronic properties by doping is one of the defining features that make DMS promising for applications. Here, we focus on the doping effect which allows the spin torque to vary as a function of hole carrier concentration. In Fig. 4(a), the torque is plotted as a function of the hole concentration for different  $\beta$  parameters. With the increase of the hole concentration, the torque increases due to an enhanced Fermi energy. In the weak spin-orbit coupling regime (small  $\beta$ ), the torque as a function of the hole concentration ( $p$ ) follows roughly the  $p^{1/3}$  curve as shown in the inset in Fig. 4(a). The spherical Fermi sphere approximation and a simple parabolic dispersion relation allow for an analytical expression of the spin torque, i.e., in the leading order

in  $\beta$  and  $J_{\text{ex}}$ ,

$$T = \frac{m^* \beta J_{\text{ex}}}{\hbar E_F} \sigma_D \quad (10)$$

where  $m^*$  is the effective mass. The Fermi energy  $E_F$  and the Drude conductivity are given by

$$E_F = \frac{\hbar^2}{2m^*} (3\pi^2 p)^{2/3}, \quad \sigma_D = \frac{e^2 \tau}{m^* p}, \quad (11)$$

where  $\tau$  is the transport time. The last two relations immediately give rise to  $T \propto p^{1/3}$ . In the six-band model, the Fermi surface deviates from a sphere and, as the value of  $\beta$  increases, the spin-orbit coupling starts to modify the density of states. Both effects render the torque-versus-hole concentration curve away from the  $p^{1/3}$  dependence. This effect is illustrated in Fig. 4(b). The former (strong spin-orbit coupling) clearly deviates from  $p^{1/3}$ , whereas the latter (weak spin-orbit coupling) follows the expected  $p^{1/3}$  trend.

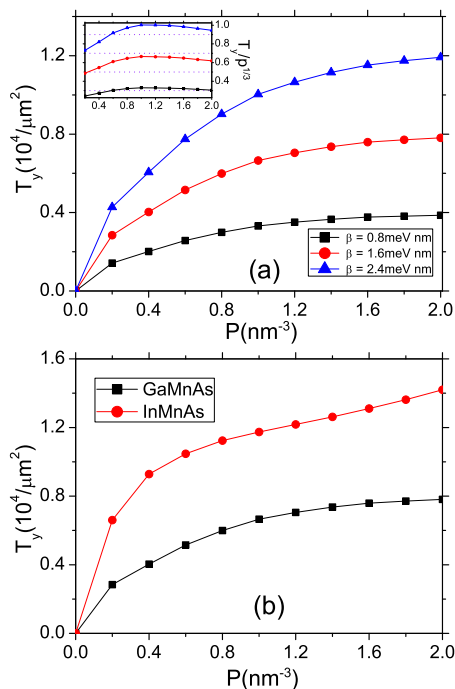


FIG. 4. (Color online) The y-component of the spin torque as a function of hole concentration. (a) The y-component of the spin torque versus hole concentration at different  $\beta$ . (b) spin torque versus hole concentration in (Ga,Mn)As and (In,Mn)As. For (Ga,Mn)As,  $J_{\text{pd}} = 55 \text{ meV nm}^3$ ; for (In,Mn)As,  $J_{\text{pd}} = 39 \text{ meV nm}^3$ . The other parameters are the same as in Fig.3.

In conclusion, in a DMS system subscribing to a linear Dresselhaus spin-orbit coupling, we have found that the angular dependence of the spin-orbit torque has a strong yet intriguing correlation with the anisotropy of the Fermi surface. Our study also reveals a nonlinear dependence of the spin torque on the exchange coupling. From the perspective of material selection, for an equivalent set of parameters, the critical switching current needed in (In,Mn)As is expected to be lower than that in (Ga,Mn)As. The results reported here shed light on the design and applications of spintronic devices based on DMS.

Whereas the materials studied in this work have a Zinc-Blende structure, DMS adopting a wurtzite structure, such as (Ga,Mn)N, might also be interesting candidates for spin-orbit torque observation due to their sizable bulk Rashba spin-orbit coupling. However, these materials usually present a significant Jahn-Teller distortion that is large enough to suppress the spin-orbit coupling.<sup>22</sup> Furthermore, the formalism developed here applies to systems possessing delocalized holes and long range Mn-Mn interactions and is not adapted to the localized holes controlling the magnetism in (Ga,Mn)N.

We are indebted to K. Výborný and T. Jungwirth for numerous stimulating discussions. F.D. acknowledges support from KAUST Academic Excellence Alliance Grant N012509-00.

\* aurelien.manchon@kaust.edu.sa

<sup>1</sup> J. A. Katine, F. J. Albert, R. A. Buhrman, E. B. Myers, and D. C. Ralph, Phys. Rev. Lett. **84**, 3149 (2000).  
<sup>2</sup> J. Slonczewski, J. Magn. Magn. Mater. **159**, L1 (1996).  
<sup>3</sup> L. Berger, Phys. Rev. B **54**, 9353 (1996).  
<sup>4</sup> A. Manchon and S. Zhang, Phys. Rev. B **78**, 212405 (2008); Phys. Rev. B **79**, 212405 (2009).  
<sup>5</sup> I. Garate and A. H. MacDonald, Phys. Rev. B **80**, 134403 (2009).  
<sup>6</sup> K. M. D. Hals, A. Brataas and Y. Tserkovnyak Eur. Phys. Lett. **90**, 47002 (2010).

<sup>7</sup> A. Chernyshov, M. Overby, X. Liu, J. K. Furdyna, Y. Lyanda-Geller, and L. P. Rokhinson, Nature Phys. **5**, 656 (2009).  
<sup>8</sup> M. Endo, F. Matsukura, and H. Ohno, Appl. Phys. Lett. **97**, 222501 (2010).  
<sup>9</sup> D. Fang, H. Kurebayashi, J. Wunderlich, K. Výborný, L. P. Zárbo, R. P. Campion, A. Casiraghi, B. L. Gallagher, T. Jungwirth, and A. J. Ferguson, Nature Nanotech. **6**, 413 (2011).  
<sup>10</sup> U. Welp, V. K. Vlasko-Vlasov, X. Liu, J. K. Furdyna, and T. Wojtowicz, Phys. Rev. Lett. **90**, 167206 (2003).

- <sup>11</sup> B. A. Bernevig and S.-C. Zhang, *Phys. Rev. B* **72**, 115204 (2005).
- <sup>12</sup> T. Jungwirth, M. Abolfath, J. Sinova, J. Kučera, and A. H. MacDonald, *Appl. Phys. Lett.* **81**, 4029 (2002).
- <sup>13</sup> M. Abolfath, T. Jungwirth, J. Brum, and A. H. MacDonald, *Phys. Rev. B* **63**, 054418 (2001).
- <sup>14</sup> J. van Bree, P. M. Koenraad, and J. Fernández-Rossier, *Phys. Rev. B* **78**, 165414 (2008).
- <sup>15</sup> A. W. Rushforth, K. Výborný, C. S. King, K. W. Edmonds, R. P. Campion, C. T. Foxon, J. Wunderlich, A. C. Irvine, P. Vašek, V. Novák, K. Olejník, Jairo Sinova, T. Jungwirth, and B. L. Gallagher, *Phys. Rev. Lett.* **99**, 147207 (2007).
- <sup>16</sup> H. Ohno, H. Munekata, T. Penney, S. von Molnár, and L. L. Chang, *Phys. Rev. Lett.* **68**, 2664 (1992).
- <sup>17</sup> S. Koshihara, A. Oiwa, M. Hirasawa, S. Katsumoto, Y. Iye, C. Urano, H. Takagi, and H. Munekata, *Phys. Rev. Lett.* **78**, 4617 (1997).
- <sup>18</sup> T. Jungwirth, Qian Niu and A. H. MacDonald, *Phys. Rev. Lett.* **88**, 207208 (2002).
- <sup>19</sup> J. Fabian, A. Matos-Abiague, C. Ertler, P. Stano, and I. Zutic, *Acta Phys. Slov.* **57**, 565 (2007).
- <sup>20</sup> H. Ohno, *J. Magn. Magn. Mater.* **200**, 110 (1999).
- <sup>21</sup> J. Wang, Master's thesis (Rice University, Houston, Texas, 2002).
- <sup>22</sup> A. Stroppa and G. Kresse, *Phys. Rev. B* **79**, 201201 (2009).